Journal of Hazardous Materials 285 (2015) 236–244

Contents lists available at ScienceDirect

Journal of Hazardous Materials

journal homepage: www.elsevier.com/locate/jhazmat

Transport, fate, and stimulating impact of silver nanoparticles on the removal of Cd(II) by *Phanerochaete chrysosporium* in aqueous solutions

Yanan Zuo[a,b], Guiqiu Chen[a,b,*], Guangming Zeng[a,b,*], Zhongwu Li[a,b], Ming Yan[a,b], Anwei Chen[c], Zhi Guo[a,b], Zhenzhen Huang[a,b], Qiong Tan[a,b]

[a] College of Environmental Science and Engineering, Hunan University, Changsha 410082, PR China
[b] Key Laboratory of Environmental Biology and Pollution Control (Hunan University), Ministry of Education, Changsha 410082, PR China
[c] College of Resources and Environment, Hunan Agricultural University, Changsha 410128, PR China

HIGHLIGHTS

- Appropriate concentration of AgNPs can stimulate the biological removal of Cd(II).
- Added AgNPs were oxidatively dissolved and transported to the surface of fungus.
- AgNPs have undergone coarsening in the process of transport.
- Amino, carboxyl, hydroxyl, and other reducing groups were involved in transportion.

GRAPHICAL ABSTRACT

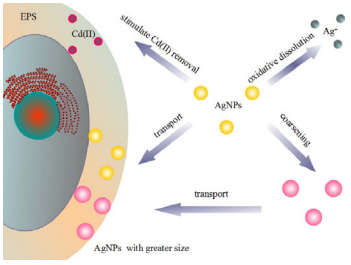

ARTICLE INFO

Article history:
Received 21 August 2014
Received in revised form 6 November 2014
Accepted 4 December 2014
Available online 5 December 2014

Keywords:
Silver nanoparticles
Cadmium
Biological removal
White-rot-fungus
Transport

ABSTRACT

Despite the knowledge about increasing discharge of silver nanoparticles (AgNPs) into wastewater and its potential toxicity to microorganisms, the interaction of AgNPs with heavy metals in the biological removal process remains poorly understood. This study focused on the effect of AgNPs (hydrodynamic diameter about 24.3 ± 0.37 nm) on the removal of cadmium (Cd(II)) by using a model white rot fungus species, *Phanerochaete chrysosporium*. Results showed that the biological removal capacity of Cd(II) increased with the concentration of AgNPs increasing from 0.1 mg/L to 1 mg/L. The maximum removal capacity (4.67 mg/g) was located at 1 mg/L AgNPs, and then decreased with further increasing AgNPs concentration, suggesting that an appropriate concentration of AgNPs has a stimulating effect on the removal of Cd(II) by *P. chrysosporium* instead of an inhibitory effect. Results of Ag^+ and total Ag concentrations in the solutions together with those of SEM and XRD demonstrated that added AgNPs had undergone oxidative dissolution and transported from the solution to the surface of fungal mycelia (up to 94%). FTIR spectra confirmed that amino, carboxyl, hydroxyl, and other reducing functional groups were involved in Cd(II) removal, AgNPs transportation, and the reduction of Ag^+ to AgNPs.

1. Introduction

Nanoparticles are defined as materials with at least two or three dimensions between 1 and 100 nm and materials in this size rang have specific mechanical, optical, electronic, and catalytic properties which are different from those of their respective bulk materials [1]. Recently, silver nanoparticles (AgNPs) have received considerable attention in the manufacturing of nanotechnology-based consumer products because of their distinctive properties [2]. According to the Project on Emerging Nanotechnologies (PEN), Ag ranks the first among the most prevalent nanomaterials in consumer products [3]. AgNPs are currently used in a variety of medical and consumer products, including suture threads, surgical blades

* Corresponding authors. Tel.: +86 731 88822829; fax.: +86 731 88823701.
E-mail addresses: gqchen@hnu.edu.cn (G. Chen), zgming@hnu.edu.cn (G. Zeng).

http://dx.doi.org/10.1016/j.jhazmat.2014.12.003
0304-3894/

[4], textiles, and personal care products, owing to their special antimicrobial, antiviral, and antifungal properties [5–7].

Concurrent with the increase in the production and application of AgNPs, the release of AgNPs into the environment is inevitable during the processes of design, usage, and disposal [1,8]. AgNPs are thus likely existed in the wastewater of sewage treatment plants (STPs) [9], thereby affecting the normal wastewater processing. So, removal of ubiquitous heavy metals in the sewage treatment unit may also be affected by the discharge of AgNPs into STPs.

However, information about the composite effect of nanoparticles and heavy metals in the literature is limited. The currently published reports are mostly concerned with the removal of heavy metals (such as Hg^{2+}, Pb^{2+}, Co^{2+}, and so on) from wastewater using $Au@SiO_2$, $Fe_3O_4@SiO_2$, and other functionalized nanoparticles [10,11] or some metal nanoparticles (such as AgNPs and AuNPs) act as a sensor for the detection of Hg^{2+}, Cu^{2+}, and other heavy metals [12,13]. And previous studies on AgNPs have mostly focused on their toxicity to different organisms [14–16] and the exploration of their toxic mechanism [17,18]. Consequently, little is known about the influence of AgNPs on the biological removal of heavy metals from wastewater.

The aim of this study was to investigate the effects of AgNPs on the removal of heavy metals by microorganisms. Cd(II) was selected as the typical heavy metal in STPs because of its widespread discharge from the industrial process of electroplating, battery manufacturing, and mineral processing [19,20]. *Phanerochaete chrysosporium* (*P. chrysosporium*), the model species of white-rot fungi, was selected as the testing microorganism as it can tolerate Cd(II) to certain degree (2–30 mg/L) and remove them effectively from wastewater (maximum of 84%) according to our previous studies [21].

To the best of our knowledge, this is the first report of the effects of AgNPs on the removal of Cd(II) from aqueous solutions by *P. chrysosporium.* In this study, AgNPs were synthesized in the laboratory and characterized by Ultraviolet–visible (UV–vis) spectrophotometry, dynamic light scattering (DLS), transmission electron microscopy (TEM), and X-ray diffraction (XRD). In order to investigate the influence of AgNPs on the removal of Cd(II) by *P. chrysosporium* and the dissolution and transport of AgNPs, the concentrations of Cd(II), Ag^+, and total Ag (including Ag^+ and AgNPs) in the solutions were determined respectively. The pH values of the solution and concentrations of extracellular proteins of *P. chrysosporium* were also analyzed in this research. These data together with the results from scanning electron microscopy (SEM), Fourier transform infrared spectrometry (FTIR), and XRD facilitated clarification of the mechanisms involving in the removal of Cd(II), the release of Ag^+, and the transport of AgNPs in the solutions.

2. Materials and methods

2.1. Synthesis and characterization of AgNPs

Citrate stabilized AgNPs were prepared in this study. This kind of particles was selected because it could be found in consumer products popularly and would be released into wastewater streams.The citrate coated AgNPs were synthesized following a protocol adapted from He et al. [14] with little modification about the stirring rate. In the process of ice bath and room temperature stirring of 3 h, the stirring rate was 540 r/min.

The citrate AgNPs suspensions were prepared daily. Several prepared AgNPs, which were synthesized in the same conditions and in the same day, were concentrated into a stock solution using centrifugal ultrafiltration (Amicon Ultra-15 3K, Millipore, USA). And the real concentration of AgNPs stock solutions were measured by flame atomic absorption spectrometry (AAS700, PerkinElmer, USA) after HNO_3 digestion. AgNPs concentrations used in this research were prepared by diluting the stock solutions to the desired concentrations. The dissolved fraction of the AgNPs stock solution was <1% as determined by analyzing the filtrate of ultrafiltration centrifuged stock suspension (Amicon Ultra-0.5 3K centrifugal tube, Millipore) using ICP-OES (IRIS Intrepid II XSP, Thermo Electron Corporation, USA).

The UV absorption spectrum of the stock AgNPs suspensions was measured using a UV–vis light spectrophotometer with the wavelength from 300 to 700 nm (Model UV-2550, Shimadzu, Japan). AgNPs size distributions were determined using a Zetasizer Nanoseries (Malvern Instruments) with a 633 nm laser source and a detection angle of 173°. The surface charge of AgNPs was evaluated with the same instrument.

Morphology of citrate coated AgNPs was characterized by transmission electron microscope on a JEOL JEM-3010 (JEOL, Japan) at 120 kV equipped with an energy dispersive X-ray (EDAX) attachment. TEM samples were prepared by placing a drop of stock AgNPs suspension onto a carbon-coated copper grid and dried at room temperature overnight. A probe sonicator (SCIENTZ-IID, Ningbo, China) was used to suspended citrate coated AgNPs in double deionized water (DDI, 18.25 MΩ cm) in ice bath as described by Meyer et al. [15].

XRD analysis of the synthesized AgNPs was conducted to further identify the formation of AgNPs in this research. The samples were prepared by concentrating the AgNPs stock solution with a centrifugal apparatus (H-1850, Dongwang, China) and vacuum drying the concentrated sampled with an electric vacuum drying oven (DZF, Yongguangming, Beijing, China). Then samples were analyzed with an automatic X-ray diffractometer (D8 Discover-2500, Bruker, German).

2.2. Microorganism and chemicals

The white-rot fungal strain *P. chrysosporium* (BKMF-1767) used in this study was obtained from the Chinese Typical Culture Center of Wuhan University (Wuhan, China). Stock cultures were maintained at 4 °C on malt extract agar slants. Mycelial suspensions were prepared in sterile distilled water, and the spore concentration was adjusted to 2.0×10^6 CFU/mL using a turbidimeter (WGZ-200, Shanghai, China). *P. chrysosporium* aqueous suspensions were prepared by transferring the fungal spores to Kirk's liquid culture medium [22] in 500 mL Erlenmeyer flasks. Then flasks containing fungal spores were incubated in an incubator under150 r/min for 3 days at 37 °C.

1 g/L Cd(II) solution was prepared as the experimental stock solution via dissolving $Cd(NO_3)_2{\cdot}4H_2O$ in ultrapure water. The exact concentration of the Cd(II) stock solution was determined by AAS. All the chemicals used in this study were analytical reagent grade. Test solutions were prepared by diluting the stock solutions to the desired concentrations. The pH value of the solution in this study, determined by a pH meter (FE20 Mettler Toledo, Switzerland), was adjusted by 0.1 mol/L NaOH or HNO_3 solutions.

2.3. Experimental procedures

After three days of incubation, the pH of *P. chrysosporium* aqueous suspension was adjusted to 6.5 with 0.1 mol/L NaOH or HNO_3 using a pH meter according to our previous study [21]. Several milliliters of Cd(II) solution were added to the flasks to ensure the final concentration of 5 mg/L. AgNPs concentrations used in the experiments were 0.1, 1, 5, 10, and 30 mg/L. Several milliliters of AgNPs were added to the solutions respectively. Flasks containing 5 mg/L Cd(II) without AgNPs were used as the control. All flasks

were incubated at 37 °C in an incubator under150 r/min. Three replicates were performed for each treatment.

2.3.1. Detection of pH values, dissolved protein content, and Cd(II) concentration

Aliquot samples were collected from the flasks at specific time intervals (2, 4, 6, 9, 12, 24, 36, 48, 60, 72, and 84 h) and used for the detection of dissolved protein content, concentrations of Cd(II), Ag^+, and total Ag. The pH values of the solution were also measured using a laboratory pH meter. Content of the dissolved protein in extracellular medium was determined via the Coomassie Brilliant Blue method with UV–vis spectrophotometer (UV754N, Shanghai, China) at 595 nm [21]. Samples were centrifuged at 10, 000 r/min for 10 min, and the supernatant was used for analyzing the residual Cd(II) in the solutions by AAS.

2.3.2. Concentrations of Ag^+ and total Ag in the solution

Concentrations of Ag^+ and total Ag were determined using ICP-OES with different treatment of the collected samples. To determine the concentrations of Ag^+, samples were firstly filtered with 0.22 μm filter membrane and centrifuged with ultrafiltration centrifuge (Amicon Ultra-0.5 3K, Millipore, USA) [23]. Then the filtrate was acidified with HNO_3 and measured with ICP-OES. Total Ag was defined as the concentration of all Ag species originating from the AgNPs. To obtain the concentration of total Ag in the solutions, the collected samples were digested with nitric acid and H_2O_2 according to the procedures of Cornelis et al. [24] and then the digested samples were used for the determination of total Ag using ICP-OES.

2.4. Characterizations of fungi after experiment

Pellets of *P. chrysosporium* were harvested by filtering after 3 days of incubation and were defined as the native fungus. Mycelium pellets in the control were collected with the same procedure after the experiment. Pellets in flasks with 5 mg/L Cd(II) and different content of AgNPs were also filtered after experiment and used as the experimental samples. All the harvested pellets were washed three times with sterile distilled water and then dried at −40 °C in a freezer dryer (FD-1, Boyikang, Beijing, China). Three kinds of dry fungal pellets from native fungus, control, and the flasks with AgNPs and Cd(II) were used for the following studies.

2.4.1. SEM analysis

In order to measure the surface characteristics of the three kinks of freeze-dried fungus, SEM (FEI QUANTA-200, FEI, USA) equipped with an EDAX attachment instrument was used. Scanning transmission electron microscopy (STEM) analysis in high-angle annular dark field (HAADF) mode was used to investigate whether physical or chemical transformation of AgNPs had occurred in the solution. Freeze-dried fungal pellets collected from the solution with Cd(II) and AgNPs were ground in mortar with methanol [25]. A drop of the ground solution was transferred to a carbon-coated copper grid and dried at room temperature overnight. Micrographs were obtained using Tecnai G^2 F20 S-TWIN (STEM, FEI, USA) coupled with an EDAX system.

2.4.2. FTIR and XRD analysis

For FTIR analysis, the freeze-dried mycelium pellets from the native, control, and experimental groups were powdered with mortars and the characteristic was obtained on an IR spectrophotometer (WQF-410, Beijing, China) with KBr tablet as reference. The freeze-dried cell pellets from the AgNPs-treated groups were also powdered for XRD analysis with the synthesized AgNPs as references. The patterns were recorded using an automatic X-ray diffractometer.

2.5. Statistical analysis

Removal rate and amount of removed Cd(II) by unit amount of dry mycelium (mg Cd(II) per g dry fungus) were calculated by following equations:

$$\text{Removal rate} = \left(\frac{C_0 - C}{C_0}\right) \times 100\% \quad (1)$$

$$q = \frac{V}{M} \times (C_0 - C) \quad (2)$$

where C_0 and C (mg/L) were concentrations of the initial and residual Cd(II) in the solution; q (mg/g) was the amount of removed Cd(II) by unit amount of dry mycelium pellets; V (L) was the volume of the solution; M (g) was the dry weight of filtered mycelium pellets after three days of incubation and treatment of freeze drying.

Results in this research were presented as mean of triplicate assays, and standard deviation was used to analyze experimental data. All of the data were analyzed and mapped with Origin 8.0 software.

3. Results and discussion

3.1. Characterization of synthesized AgNPs

Fig. 1A showed the UV–vis absorption spectrum of synthesized AgNPs in DDI water. The absorption peak of the synthesized citrate-coated AgNPs was 394 nm, which corresponded to the results of Liu and Hurt [26]. Synthesized AgNPs had a negative surface charge (−47.2 mV of ζ-potential). DLS results showed that the mean hydrodynamic diameters of synthesized AgNPs in DDI water was approximately 24.3 ± 0.37 nm (inset in Fig. 1B).

TEM image of synthesized AgNPs was presented in Fig. 1B. The average diameter of these particles was estimated at approximately 25.0 nm from TEM. The difference in the average particle size by the two techniques (DLS and TEM) could be due to the slight aggregation occurring during TEM sample preparation. TEM micrograph revealed that the synthesized AgNPs were spherical. The EDAX spectrum of the black spherical dots in the TEM image was shown in Fig. 1C. There was an obvious peak of Ag in the EDAX spectrum, which demonstrated that the black dots in TEM image contained Ag.

The XRD pattern of synthesized AgNPs exhibited prominent broad peaks at 2θ values of 38.1°, 44.09°, 64.36°, and 77.29° (Fig. 1D), which could be assigned to the diffraction signals of (1 1 1), (2 0 0), (2 2 0), and (3 1 1) facets of Ag, respectively, with reference to Vigneshwaran et al. [27]. Coupled with above results, it could be concluded that AgNPs had been successfully synthesized in this research.

3.2. Effects of AgNPs on the removal of Cd(II)

To understand the effects of AgNPs on Cd(II)-removal efficiency, Cd(II) concentrations in the solution were determined at indicated time intervals. The results were presented in terms of biological removal capacity in Fig. 2. It could be seen from Fig. 2 that the initial concentrations of AgNPs significantly influenced the Cd(II) removal capacity. The removal capacity of Cd(II) increased with the increasing of initial AgNPs concentration from 0.1 to 1 mg/L. And the maximum removal capacity of Cd(II) (4.67 mg/g) was achieved at an initial AgNPs concentration of 1 mg/L.

AgNPs, as a new kind of pollutant, have been reported to be toxic to a variety of microorganisms [15,16,28], algae [14], and fish [29]. However, results of this research demonstrated that the use of appropriate concentration of AgNPs had a promotional effect on the removal efficiency of Cd(II) from the solution by *P. chrysosporium* rather than inhibited the activity of fungus. The removal efficiency

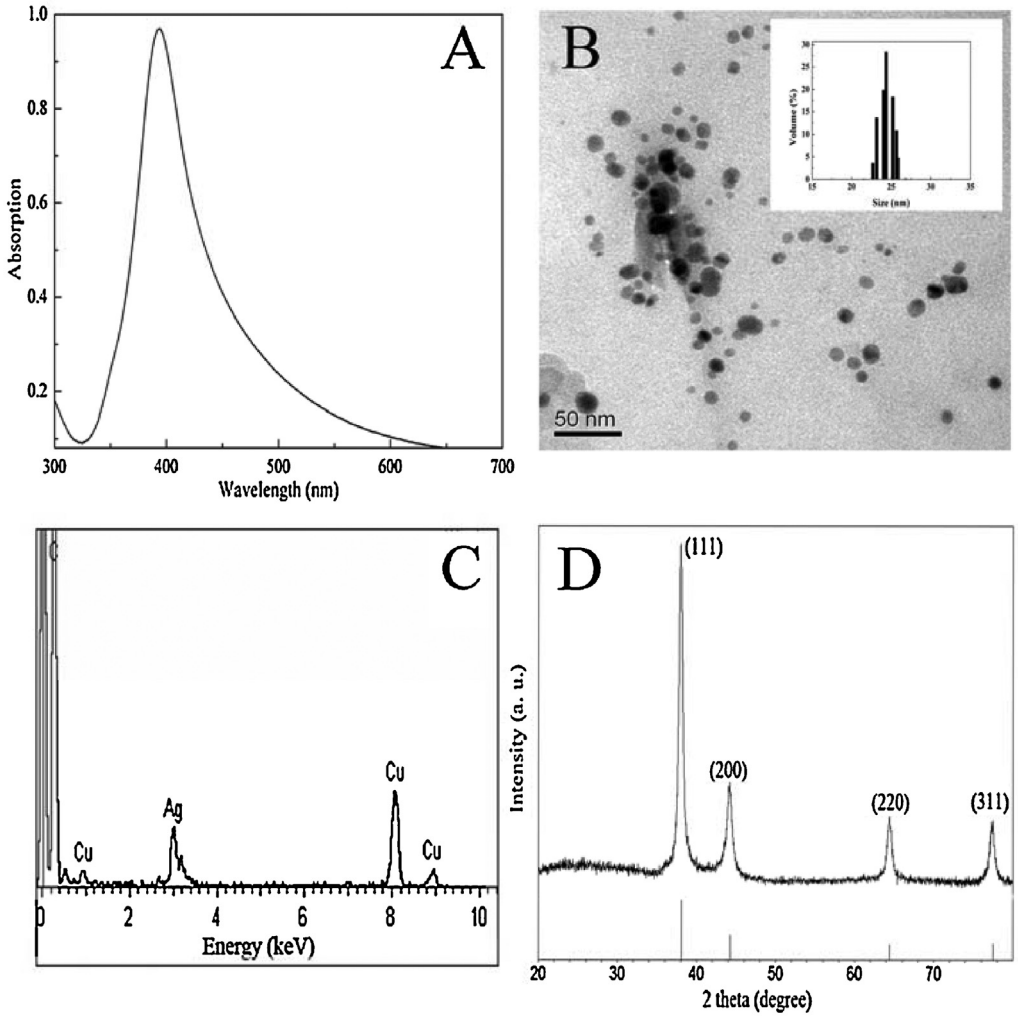

Fig. 1. Characterization of synthesized AgNPs: (A) UV–vis absorption spectrum. (B) TEM image. Inset at the right corner gave hydrodynamic diameters of synthesized AgNPs. (C) EDAX analysis of the black spherical dots in TEM image. (D) X-ray diffraction.

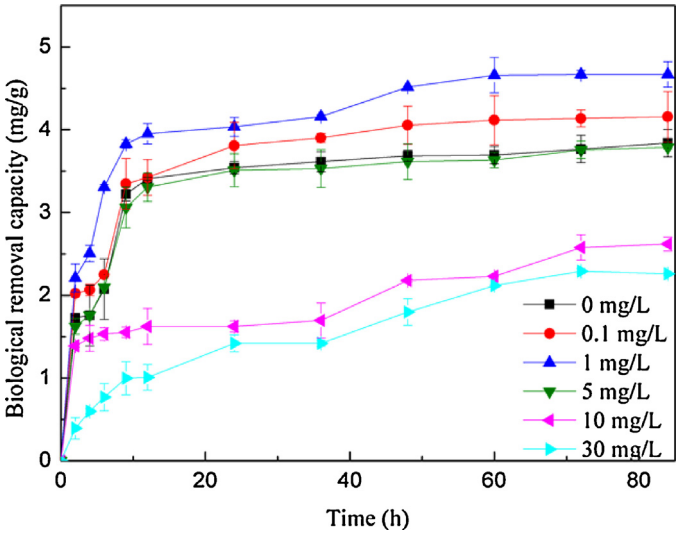

Fig. 2. Biological removal capacity of *P. chrysosporium* to 5 mg/L Cd(II) in the present of different concentrations of AgNPs.

of Cd(II) decreased with the concentration of added AgNPs further increasing to 5, 10, and 30 mg/L (Fig. 2). These results indicated that use of a higher concentration of AgNPs may suppress the Cd(II)-removal efficiency of *P. chrysosporium* instead of stimulate it.

The positive effect of AgNPs to the removal of Cd(II) by *P. chrysosporium* can be attributed to the overcompensatory behavior of microorganisms. Xiu et al. [18] have reported that a sublethal concentration of AgNPs can stimulate the survival of *Escherichia coli* and hinder antimicrobial applications due to activation of repair mechanism of the cells against toxicant under low dose of AgNPs, which may overcompensate for the toxic exposure. Similar stimulatory effects at low doses of AgNPs have also been observed in biofilms treated with AgNPs [30]. In this study, the maximum removal capacity of Cd(II) occurred at an initial added AgNP concentration of 1 mg/L, which is a relatively low dose to *P. chrysosporium* compared to the higher concentrations of 5, 10, and 30 mg/L. This low concentration of AgNPs may motivate the overcompensatory mechanism of *P. chrysosporium*, thus stimulating the removal of Cd(II) from the aqueous solutions.

Our previous study has demonstrated that *P. chrysosporium* may secrete extracellular protein upon exposure to heavy metals [21]. In the present study, the results of extracellular protein content (Table 1) indicate the presence of abundant protein in the solution. Relative literature reported that natural organic matter (NOM) may cause the surface of AgNPs to be more negatively charged, some-

Table 1
Extracellular protein concentrations of *P. chrysosporium* during incubation.

AgNPs concentration (mg/L)	0 h	2 h	4 h	6 h	9 h	12 h	24 h	36 h	48 h	60 h	72 h	84 h
0	0.243	0.217	0.210	0.193	0.164	0.162	0.206	0.256	0.278	0.267	0.259	0.278
0.1	0.230	0.205	0.202	0.188	0.142	0.094	0.113	0.129	0.134	0.139	0.149	0.150
1	0.225	0.184	0.175	0.181	0.153	0.138	0.176	0.214	0.255	0.242	0.246	0.247
5	0.191	0.168	0.156	0.137	0.140	0.152	0.185	0.212	0.215	0.210	0.223	0.229
10	0.239	0.208	0.216	0.204	0.240	0.249	0.269	0.287	0.289	0.277	0.277	0.276
30	0.254	0.230	0.227	0.219	0.237	0.229	0.252	0.279	0.280	0.283	0.286	0.287

what decreasing inhibitory effects of AgNPs on bacterial growth [31]. The presence of large amounts of functional groups such as carboxyl, amino, and hydroxyl groups in the extracellular protein has similar effect as that of NOM to AgNPs. Electrostatic repulsion between AgNPs and the negatively charged fungal cell wall can therefore reduce the toxicity of AgNPs to the fungus. However, the inhibitory effect of AgNPs to the fungus may intensify when the increased concentration of AgNPs exceeded the amount of functional groups of proteins provided by the fungus, which may weaken the stimulatory effect of AgNPs on the removal of Cd(II) with the concentration of AgNPs increasing from 1 to 30 mg/L.

Ag^+ released from the crystalline core of AgNPs is the major factor responsible for the toxicity of nanomaterials [18]. It has been reported that NOM can also bind with the bioavailable Ag^+ [30]. NOM-like extracellular protein provided by the fungus may combine with the released Ag^+ to decrease the toxicity of AgNPs on microorganisms. Our previous studies have reported that *P. chrysosporium* may secrete extracellular polymeric substances (EPS) during their exposure to toxic substance [32]. EPS can act as a barrier to antimicrobial transport of AgNPs into the microbial cells and avoid direct contact of AgNPs with the cell [30], reducing the toxicity of AgNPs on the microorganisms.

3.3. Oxidative dissolution and transport of AgNPs

3.3.1. Oxidative dissolution of AgNPs

Ag^+ was derived from the dissolved AgNPs. Fig. 3A demonstrated that the dissolution rate of added AgNPs increased rapidly in the first 12 h for all concentrations of AgNPs, and reached a plateau at about 36 h. Ag^+ can be released from AgNPs following oxidation of Ag (0) on the nanoparticles surface:

$$4Ag^0 + O_2 \rightarrow 2Ag_2O \quad (3)$$

$$2Ag_2O + 4H^+ \rightarrow 4Ag^+ + 2H_2O \quad (4)$$

The equations given above indicate the necessity of oxygen in the dissolution process of AgNPs. Because of flasks in this experiment were incubated under rotation of 150 r/min, there was an excess of dissolved oxygen in the system, which could accelerate the oxidative dissolution of AgNPs.

Previous studies suggested that low pH environment can promote the dissolution of metal nanoparticles [26,33]. The pH values of the solution in this study decreased during the incubation process (Table 2) probably due to the production of organic acids such as oxalic acid during the metabolic process of the fungus [34]. The decreased pH value of the solution may account for the increase of Ag^+ concentration in the solution.

Release of Ag^+ can be highly variable in the presence of microorganisms. The metabolic state of microbes can affect the dissolved oxygen concentration and pH of the solution, remove the polymeric substances coating AgNPs, and increase the Ag-dissolution gradient by binding the released Ag^+ [5,18,31]. Therefore, the dissolution of AgNPs may be affected by the metabolic state of *P. chrysosporium* in this study.

Release of Ag^+ can be restrained by coating the citrate-capped AgNPs with humic acid (HA, a typical NOM) [26]. In addition, HA could adsorb to the surface of nanoparticles and block surface sites to hinder the dissolution of nanoparticles [26]. As mentioned above, *P. chrysosporium* can secrete some organic acids such as oxalic acid during its metabolic process which may act like HA and hinder further dissolution of AgNPs. Insufficient dissolution of AgNPs resulted in a plateau of Ag^+ concentration in the solution at approximately 36 h, with no further increase in the concentration. Moreover, Ag^+ can bind strongly with organosulfur compounds, with the greatest affinity for thiol-containing ligands [33]. *P. chrysosporium* may produce organosulfur compounds such as glutathione due to oxidative stress [35] or exposure to toxic Cd(II) and AgNPs. These organosulfur compounds may also contribute to the suppression of further dissolution of AgNPs in this system.

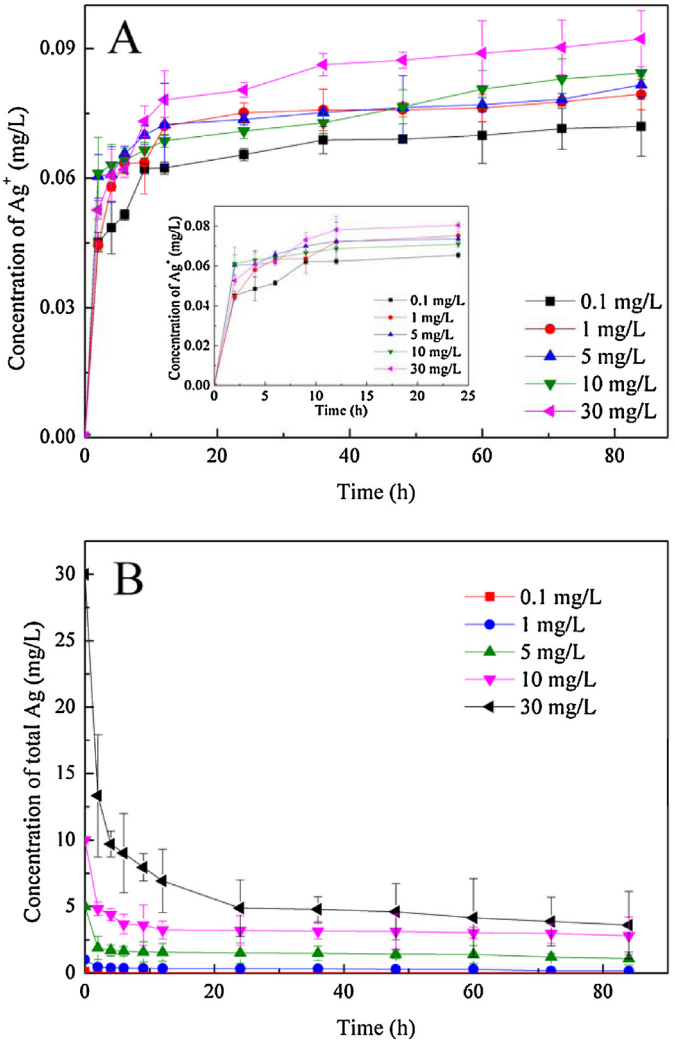

Fig. 3. (A) Concentrations of Ag^+ in the solutions. Inset gave enlarged view of results from 0 to 24 h. (B) Changes of total Ag concentrations in solutions.

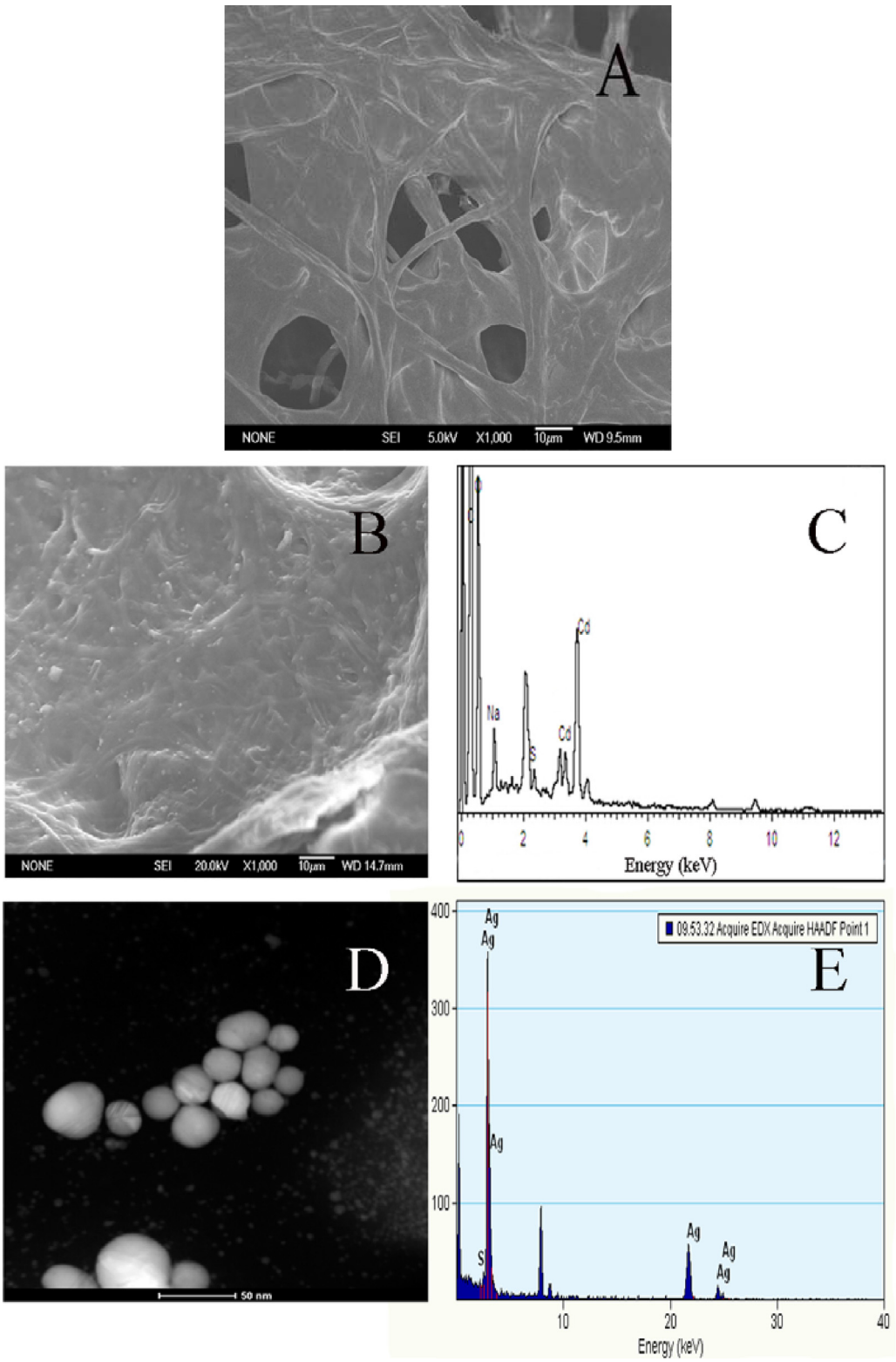

Fig. 4. SEM and EDAX analysis: (A) SEM image for native fungal pellets (B) SEM spectrum for fungal cell pellets in control. (C) EDAX analysis for particles appeared in Fig. 4B. (D) HAADF-STEM image of freeze-dried fungal pellets from AgNPs-treated samples. (E) EDAX spectrum for the bright spots appeared in Fig. 4D.

Table 2
Changes of pH values of the solution.

AgNPs concentration (mg/L)	0 h	2 h	4 h	6 h	9 h	12 h	24 h	36 h	48 h	60 h	72 h	84 h
0	6.52	7.13	7.17	7.17	6.92	7.36	7.11	6.10	4.91	4.71	4.00	3.86
0.1	6.52	6.94	6.96	7.03	6.87	5.15	5.09	5.12	4.53	4.30	4.02	4.15
1	6.51	7.02	7.05	7.07	6.99	5.23	5.34	5.13	5.13	4.68	3.80	3.90
5	6.52	7.25	7.21	7.18	7.11	5.74	5.13	5.08	5.04	4.29	3.75	3.85
10	6.49	7.16	7.22	7.23	7.42	7.17	5.04	5.13	4.90	4.13	3.86	4.01
30	6.51	6.72	6.78	6.77	6.68	6.55	5.03	4.88	4.82	4.33	3.83	3.84

3.3.2. Transport of AgNPs in the solutions

The total Ag content was defined as the concentration of all Ag species (including Ag^+ and AgNPs) originating from the initial AgNPs. Changes in the total Ag content in the solutions during the experiment were illustrated in Fig. 3B. The concentration of total Ag decreased for all concentrations of AgNPs, demonstrating that AgNPs and other forms of Ag were transferred from the solution phase to the biological phase. The transportation rates of all forms of Ag were 94%, 85%, 78%, 72%, and 88% at the initial AgNPs concentrations of 0.1, 1, 5, 10, and 30 mg/L, respectively. In addition, transport of AgNPs occurred more rapidly during the first 24 h for all AgNP-treated samples.

As the total Ag content was contributed by all Ag species originating from the added AgNPs, the final concentration of total Ag in the solution was affected by the decrease in the concentration of Ag^+ and AgNPs. Previous analysis had indicated that release of Ag^+ could be inhibited by the action of organic acids and organosulfur compounds secreted by *P. chrysosporium*. In aquatic system, NOM played an important role in determining the environmental fate and transport of AgNPs by influencing the physicochemical properties and thereby altering the agglomeration, bioavailability, and toxicity of AgNPs [36]. Biomacromolecules (such as extracellular proteins listed in Table 1) produced by *P. chrysosporium* were similar to NOM in their functional groups (such as hydroxyl and amino). Complexation of Ag^+ and AgNPs with biomacromolecules secreted by the fungus and the binding of AgNPs with the functional groups on the fungus cell wall (further explained in Section 3.4.3) together decreased the concentration of total Ag in the solutions.

3.4. Mechanism exploration for the removal of Cd(II) and the transport of AgNPs

3.4.1. SEM–EDAX analysis

Dry mycelial pellets (native and cells in the control groups) were analyzed by SEM and EDAX to obtain a better understanding of Cd(II) removal. As shown in Fig. 4A, the surface of the native fungus appeared smooth and clean without any absorbed particles, while several particles were dispersed on the control mycelial surface (Fig. 4B). The EDAX spectrum of the particles in Fig. 4B was presented in Fig. 4C. The clear peak of Cd in the EDAX spectrum demonstrated that Cd(II) was loaded on the mycelium of *P. chrysosporium*.

To gain further insight into the transport and fate of AgNPs, high-angle annular dark field scanning transmission electron microscopy (HAADF-STEM) was used for analyzing the AgNPs-treated mycelial pellets. Fig. 4D showed the typical image of biosolid loaded with nanoscale particles (bright dots) recorded on the TEM by using the HAADF detector. Further analyses of the bright spots by EDAX confirmed the presence of Ag element in these region (Fig. 4E), indicating that Ag was transferred to the biological phase.

3.4.2. XRD analysis

To better understand the existing form of Ag in the HAADF-STEM image, freeze-dried cell pellets from the flasks with Cd(II) and AgNPs were powered and used for XRD analysis. Fig. 5 showed that the characteristic peaks of the AgNPs-treated pellets (B) were identical to those of the previously synthesized AgNPs (A) and the PDF card reference. This result suggested that the bright dots on the HAADF-STEM image were AgNPs. However, the size of the AgNPs was larger comparing to that of our synthesized AgNPs, indicating that aggregation occurred during the transport process.

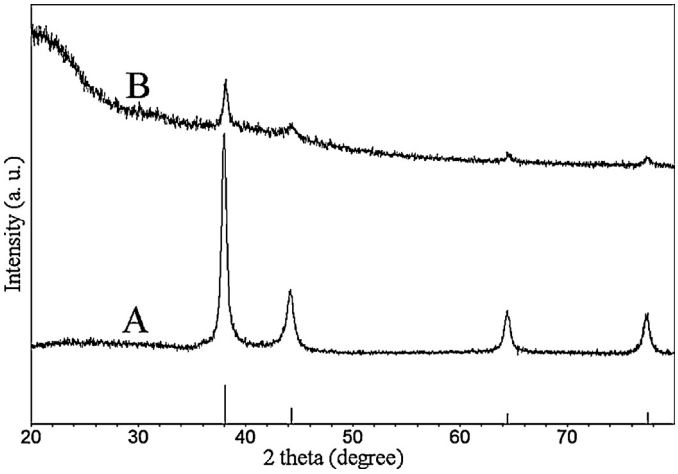

Fig. 5. XRD pattern for freeze-dried cell pellets from the AgNPs-treated samples.

However, it could not be ascertained whether the AgNPs loaded on the surface of fungal mycelia were completely contributed by the added AgNPs. Because Ag^+, released from AgNPs, can also be reduced to nanoscale zero-valent state by the reducing components in the solution. Vigneshwaran [27] reported extracellular synthesis of AgNPs by *P. chrysosporium*. The author reported that the reducing sugars derived from the saccharides were responsible for the reduction of Ag^+ to AgNPs. Therefore, AgNPs appearing on the surface of the fungus may be partially contributed by the released Ag^+ that was reduced by the reducing components produced by *P. chrysosporium*.

Akaighe et al. [37] also reported the formation of AgNPs by reduction of Ag^+ using HA at room temperature. HA contains functional groups such as hydroxyls, aldehydes, ketones, and thiols that could serve as the reduction sites for metal ions. The results of FTIR analysis (Section 3.4.3) demonstrated that similar functional groups were presented on the surface of the fungal mycelia, which may be involved in the reduction of Ag^+ to AgNPs.

3.4.3. FTIR analysis

In order to determine the functional groups responsible for the removal of Cd(II), the transport of AgNPs, and maybe the reduction of Ag^+, FTIR analysis of the fungal pellets from native, control, and AgNPs-treated groups were performed (Fig. 6).

The strong, broad infrared (IR) absorption band at 3354 cm^{-1} for the native fungus was a characteristic of the O—H stretching vibration of the carboxyl group. The characteristic peak of O—H shifted to 3414 cm^{-1} for fungus treated with Cd(II) and AgNPs, indicating that the oxygen atoms were the binding sites for Cd(II) and Ag. In addition, the reducing O—H group may be also involved in the reduction of Ag^+ to AgNPs.

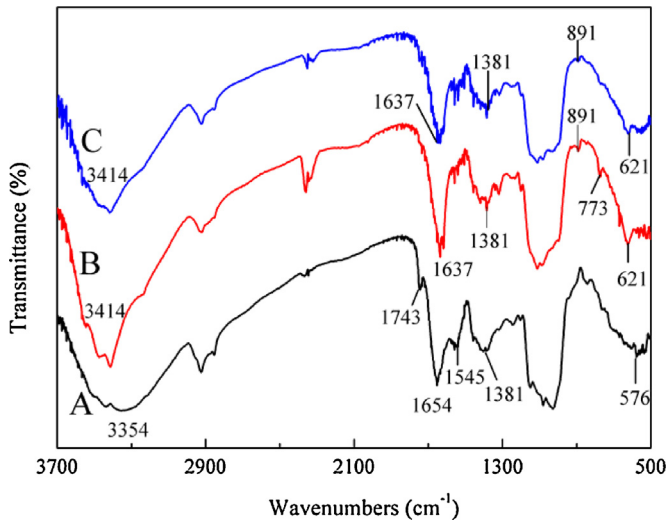

Fig. 6. FTIR analyses for freeze-dried cell pellets from native (A), control (B) and AgNPs-treated samples (C).

Within the region of 3500–3300 cm^{-1}, the N—H stretching vibration bands of the fungus may overlap with the strong and large band of the carboxyl group [38]. Both of N—H and carboxyl groups offered more binding sites for Cd(II), Ag^+, and AgNPs. Peaks at 1743 cm^{-1} and 1654 cm^{-1} were the characteristics of C=O group stretching from the aldehydes and ketones. The reduced aldehydes and ketones may be responsible for the reduction of Ag^+ to AgNPs. The absorption peak at 1743 cm^{-1} disappeared after the addition of Cd(II) and AgNPs, indicating the reaction of Cd(II), Ag^+, and AgNPs with peptide bond.

The spectra displayed two absorption bounds at 1637 cm^{-1} and 1545 cm^{-1} corresponding to the stretching vibration of amide I (C=O) and amide II (N—H) of polypeptides or proteins [39]. The weakened intensity of the 1545 cm^{-1} band in Fig. 6B and C demonstrated that N—H was involved in the removal of Cd(II) and the transport of AgNPs. The absorption peak at 1381 cm^{-1} was a characteristic of the carboxyl groups that may indicate the typical carboxyl adsorption of metal ions. In addition, peaks at 891 $cm^{-1}$and 773 cm^{-1} could be assigned to the asymmetry stretching of P—O—S and the deformation vibration of N—H, whereas the peaks appearing at 621 cm^{-1} and 576 cm^{-1} might represent stretching vibration of P—S. Cd(II) and Ag^+ may replace the sites of S and thus bonded on the surface of the fungus.

4. Conclusions

This research found that appropriate concentration of AgNPs can stimulate the removal of Cd(II) by *P. chrysosporium* in aqueous solutions instead of inhibit the activity of the fungus. This positive effect of AgNPs on biological removal of Cd(II) is a unique supplement to the toxic effects of AgNPs to microorganisms. In this study, the added AgNPs in the solutions were oxidatively dissolved and transferred from the solution to the surface of fungal mycelia (maximum of 94%). Amino, hydroxyl, and carboxyl groups as well as other reducing functional groups provided by *P. chrysosporium* played an important role in the removal of Cd(II), transport of AgNPs, and the reduction of Ag^+ to AgNPs. However, whether the total AgNPs adsorbed on the surface of fungal mycelia were fully contributed by the added AgNPs or whether some of them were contributed by Ag^+ reduced by ubiquitous reducing components in the solutions needs to be investigated in further studies.

Acknowledgment

This study was financially supported by the National Natural Science Foundation of China (51178171, 51039001, and 41271294).

References

[1] J. Farkas, P. Christian, J.A. Urrea, N. Roos, M. Hassellöv, K.E. Tollefsen, K.V. Thomas, Effects of silver and gold nanoparticles on rainbow trout (*Oncorhynchus mykiss*) hepatocytes, Aquat. Toxicol. 96 (2010) 44–52.
[2] P. Das, C.D. Metcalfe, M.A. Xenopoulos, Interactive effects of silver nanoparticles and phosphorus on phytoplankton growth in natural waters, Environ. Sci. Technol. 48 (2014) 4573–4580.
[3] R. Ma, C. Levard, J.D. Judy, J.M. Unrine, M. Durenkamp, B. Martin, B. Jefferson, G.V. Lowry, Fate of zinc oxide and silver nanoparticles in a pilot wastewater treatment plant and in processed biosolids, Environ. Sci. Technol. 48 (2014) 104–112.
[4] D.M. Eby, H.R. Luckarift, G.R. Johnson, Hybrid antimicrobial enzyme and silver nanoparticle coatings for medical instruments, ACS Appl. Mater. Interfaces 1 (2009) 1553–1560.
[5] T.V. Braga, R.M. Graff, K. Wojdyla, A. Rogowska-Wrzesinska, J.R. Brewer, H. Erdmann, F. Kjeldsen, Insights into the cellular response triggered by silver nanoparticles using quantitative proteomics, ACS Nano 8 (2014) 2161–2175.
[6] N. Joshi, B.T. Ngwenya, C.E. French, Enhanced resistance to nanoparticle toxicity is conferred by overproduction of extracellular polymeric substances, J. Hazard. Mater. 241 (2012) 363–370.
[7] C. Larue, H. Castillo-Michel, S. Sobanska, L. Cécillon, S. Bureau, V. Barthès, L. Ouerdane, M. Carrière, G. Sarret, Foliar exposure of the crop *Lactuca sativa* to silver nanoparticles: evidence for internalization and changes in Ag speciation, J. Hazard. Mater. 264 (2014) 98–106.
[8] A. García, L. Delgado, J.A. Torà, E. Casals, E. González, V. Puntes, X. Font, J. Carrera, A. Sánchez, Effect of cerium dioxide titanium dioxide, silver, and gold nanoparticles on the activity of microbial communities intended in wastewater treatment, J. Hazard. Mater. 199 (2012) 64–72.
[9] R. Kaegi, A. Voegelin, B. Sinnet, S. Zuleeg, H. Hagendorfer, M. Burkhardt, H. Siegrist, Behavior of metallic silver nanoparticles in a pilot wastewater treatment plant, Environ. Sci. Technol. 45 (2011) 3902–3908.
[10] M. Liu, Z. Wang, S. Zong, H. Chen, D. Zhu, L. Wu, G. Hu, Y. Cui, SERS detection and removal of mercury(II)/silver(I) using oligonucleotide-functionalized core/shell magnetic silica sphere@Au nanoparticles, ACS Appl. Mater. Interfaces 6 (2014) 7371–7379.
[11] K. Zargoosh, H. Abedini, A. Abdolmaleki, M.R. Molavian, Effective removal of heavy metal ions from industrial wastes using thiosalicylhydrazide-modified magnetic nanoparticles, Ind. Eng. Chem. Res. 52 (2013) 14944–14954.
[12] M. Annadhasan, T. Muthukumarasamyvel, V.R. Sankar Babu, N. Rajendiran, Green synthesized silver and gold nanoparticles for colorimetric detection of Hg^{2+} Pb^{2+}, and Mn^{2+} in aqueous medium, ACS Sustainable Chem. Eng. 2 (2014) 887–896.
[13] V.N. Mehta, M.A. Kumar, S.K. Kailasa, Colorimetric detection of copper in water samples using dopamine dithiocarbamate-functionalized Au nanoparticles, Ind. Eng. Chem. Res. 52 (2013) 4414–4420.
[14] D. He, J.J.D. Aranda, T.D. Waite, Silver nanoparticle-algae interactions: oxidative dissolution, reactive oxygen species generation and synergistic toxic effects, Environ. Sci. Technol. 46 (2012) 8731–8738.
[15] J.N. Meyer, C.A. Lord, X.Y. Yang, E.A. Turner, A.R. Badireddy, S.M. Marinakos, A. Chilkoti, M.R. Wiesner, M. Auffan, Intracellular uptake and associated toxicity of silver nanoparticles in *Caenorhabditis elegans*, Aquat. Toxicol. 100 (2010) 140–150.
[16] C.L. Arnaout, C.K. Gunsch, Impacts of silver nanoparticle coating on the nitrification potential of *Nitrosomonas europaea*, Environ. Sci. Technol. 46 (2012) 5387–5395.
[17] C.O. Dimkpa, A. Calder, P. Gajjar, S. Merugu, W. Huang, D.W. Britt, J.E. McLean, W.P. Johnson, A.J. Anderson, Interaction of silver nanoparticles with an environmentally beneficial bacterium, *Pseudomonas chlororaphis*, J. Hazard. Mater. 188 (2011) 428–435.
[18] Z.M. Xiu, Q.B. Zhang, H.L. Puppala, V.L. Colvin, P.J. Alvarez, Negligible particle-specific antibacterial activity of silver nanoparticles, Nano Lett. 12 (2012) 4271–4275.
[19] G. Chen, G. Zeng, L. Tang, C. Du, X. Jiang, G. Huang, H. Liu, G. Shen, Cadmium removal from simulated wastewater to biomass byproduct of *Lentinus edodes*, Bioresour. Technol. 99 (2008) 7034–7040.
[20] M.D. Mashitah, Y.Y. Azila, S. Bhatia, Biosorption of cadmium (II) ions by immobilized cells of *Pycnoporus sanguineus* from aqueous solution, Bioresour. Technol. 99 (2008) 4742–4748.
[21] A.W. Chen, G.M. Zeng, G. Chen, J. Fan, Z. Zou, H. Li, X. Hu, F. Long, Simultaneous cadmium removal and 2,4-dichlorophenol degradation from aqueous solutions by *Phanerochaete chrysosporium*, Appl. Microbiol. Biotechnol. 91 (2011) 811–821.
[22] G.M. Zeng, A.W. Chen, G.Q. Chen, X.J. Hu, S. Guan, C. Shang, L.H. Lu, Z.J. Zou, Responses of *Phanerochaete chrysosporium* to toxic pollutants: physiological flux, oxidative stress, and detoxification, Environ. Sci. Technol. 46 (2012) 7818–7825.

[23] R. Ma, C. Levard, F.M. Michel, G.E. Brown, G.V. Lowry, Sulfidation mechanism for zinc oxide nanoparticles and the effect of sulfidation on their solubility, Environ. Sci. Technol. 47 (2013) 2527–2534.
[24] G. Cornelis, J.K. Kirby, D. Beak, D. Chittleborough, M.J. McLaughlin, A method for determination of retention of silver and cerium oxide manufactured nanoparticles in soils, Environ. Chem. 7 (2010) 298–308.
[25] C.L. Doolette, M.J. McLaughlin, J.K. Kirby, D.J. Batstone, H.H. Harris, H. Ge, G. Cornelis, Transformation of PVP coated silver nanoparticles in a simulated wastewater treatment process and the effect on microbial communities, Chem. Cent. J. 7 (2013) 1–18.
[26] J. Liu, R.H. Hurt, Ion release kinetics and particle persistence in aqueous nano-silver colloids, Environ. Sci. Technol. 44 (2010) 2169–2175.
[27] N. Vigneshwaran, A.A. Kathe, P.V. Varadarajan, R.P. Nachane, R.H. Balasubramanya, Biomimetics of silver nanoparticles by white rot fungus, *Phaenerochaete chrysosporium*, Colloids Surf. B 53 (2006) 55–59.
[28] Y. Wang, P. Westerhoff, K.D. Hristovski, Fate and biological effects of silver titanium dioxide, and C_{60} (fullerene) nanomaterials during simulated wastewater treatment processes, J. Hazard. Mater. 201–202 (2012) 16–22.
[29] T.M. Scown, E.M. Santos, B.D. Johnston, B. Gaiser, M. Baalousha, S. Mitov, J.R. Lead, V. Stone, T.F. Fernandes, M. Jepson, R. van Aerle, C.R. Tyler, Effects of aqueous exposure to silver nanoparticles of different sizes in rainbow trout, Toxicol. Sci. 115 (2010) 521–534.
[30] S.M. Wirth, G.V. Lowry, R.D. Tilton, Natural organic matter alters biofilm tolerance to silver nanoparticles and dissolved silver, Environ. Sci. Technol. 46 (2012) 12687–12696.
[31] J. Fabrega, S.R. Fawcett, J.C. Renshaw, J.R. Lead, Silver nanoparticle impact on bacterial growth: effect of pH, concentration, and organic matter, Environ. Sci. Technol. 43 (2009) 7285–7290.
[32] G.Q. Chen, Y. Zhou, G.M. Zeng, H.Y. Liu, M. Yan, A.W. Chen, S. Guan, C. Shang, H.K. Li, J.M. He, Alteration of culture fluid proteins by cadmium induction in *Phanerochaete chrysosporium*, J. Basic Microbiol. 53 (2013) 1–7.
[33] C. Levard, E.M. Hotze, G.V. Lowry, G.E. Brown, Environmental transformations of silver nanoparticles: impact on stability and toxicity, Environ. Sci. Technol. 46 (2012) 6900–6914.
[34] D.L. Huang, G.M. Zeng, C.L. Feng, S. Hu, X.Y. Jiang, L. Tang, F.F. Su, Y. Zhang, W. Zeng, H.L. Liu, Degradation of lead-contaminated lignocellulosic waste by *Phanerochaete chrysosporium* and the reduction of lead toxicity, Environ. Sci. Technol. 42 (2008) 4946–4951.
[35] P. Xu, L. Liu, G.M. Zeng, D.L. Huang, C. Lai, M. Zhao, C. Huang, N. Li, Z. Wei, H. Wu, C. Zhang, M. Lai, Y. He, Heavy metal-induced glutathione accumulation and its role in heavy metal detoxification in *Phanerochaete chrysosporium*, Appl. Microbiol. Biotechnol. 98 (2014) 6409–6418.
[36] S. Bae, Y.S. Hwang, S.K. Lee, Effects of water chemistry on aggregation and soil adsorption of silver nanoparticles, Environ. Health Toxicol. 28 (2013) 1–15.
[37] N. Akaighe, R.I. Maccuspie, D.A. Navarro, D.S. Aga, S. Banerjee, M. Sohn, V.K. Sharma, Humic acid-induced silver nanoparticle formation under environmentally relevant conditions, Environ. Sci. Technol. 45 (2011) 3895–3901.
[38] G.Q. Chen, Z.J. Zou, G.M. Zeng, M. Yan, J.Q. Fan, A.W. Chen, F. Yang, W.J. Zhang, L. Wang, Coarsening of extracellularly biosynthesized cadmium crystal particles induced by thioacetamide in solution, Chemosphere 83 (2011) 1201–1207.
[39] J.W. Moreau, P.K. Weber, M.C. Martin, B. Gilbert, I.D. Hutcheon, J.F. Banfield, Extracellular proteins limit the dispersal of biogenic nanoparticles, Science 316 (2007) 1600–1603.